

QoS-Aware Joint Power Allocation and Task Offloading in a MEC/NFV-enabled C-RAN Network

Mohsen Tajallifar, Sina Ebrahimi, Mohammad Reza Javan, Nader Mokari,
and Luca Chiaraviglio,

Abstract

In this paper, we propose a novel resource management scheme that jointly allocates the transmission power and computational resources in a centralized radio access network architecture. The network comprises a set of computing nodes to which the requested tasks of different users are offloaded. The optimization problem takes the transmission, execution, and propagation delays of each task into account, with the aim to allocate the transmission power and computational resources such that the user's maximum tolerable latency is satisfied. Since the optimization problem is highly non-convex, we adopt the alternate search method (ASM) to divide it into smaller subproblems. A heuristic algorithm is proposed to jointly manage the allocated computational resources and placement of the tasks derived by ASM. We also propose an admission control mechanism for finding the set of tasks that can be served by the available resources. Furthermore, a disjoint method that separately allocates the transmission power and the computational resources is proposed as the baseline of comparison. The optimal solution of the optimization problem is also derived based on exhaustive search over offloading decisions and utilizing Karush–Kuhn–Tucker optimality conditions. The simulation results show that the joint method outperforms the disjoint task offloading and power allocation. Moreover, simulations show that the performance of the proposed method is almost equal to that of the optimal solution.

Index Terms

Multi-access/Mobile Edge Computing (MEC), Task Offloading, Network Function Virtualization (NFV), Admission Control, Centralized Radio Access Network (C-RAN).

M. Tajallifar, S. Ebrahimi, and N. Mokari are with the Department of Electrical and Computer Engineering, Tarbiat Modares University, Tehran, 14115-111 Iran e-mail: nader.mokari@modares.ac.ir. M. Javan is with Shahrood University of Technology. L. Chiaraviglio is with University of Rome Tor Vergata.

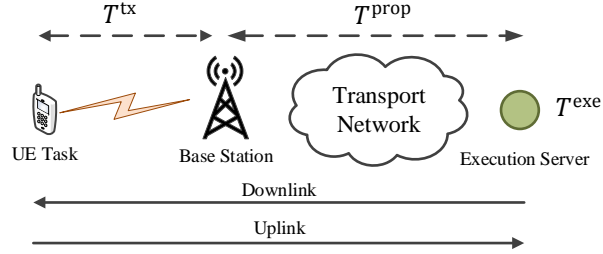


Fig. 1: A typical task offloading example.

I. INTRODUCTION

A. Background

In order to fulfill the requirements of 5G mobile networks, key enabling technologies such as network function virtualization (NFV) and multi-access/mobile edge computing (MEC) are introduced. With NFV, the network functions (NFs) that traditionally used dedicated hardware are implemented in applications running on top of commodity servers [1]. On the other hand, MEC aims to support low-latency mobile services by bringing the remote cloud servers closer to the mobile users [2], [3]. Moreover, MEC enables the offloading of the computational burden of users' tasks to reduce the impact of the limited battery power of user equipment (UE).

A typical task offloading example is shown in Fig. 1. The main idea of the task offloading is to transmit the non-processed data of a task from UE to an execution server that offloads the computational burden of the task execution on the remote server. As Fig. 1 shows, the user transmits the non-processed data of the task over the wireless link in the uplink to its serving base station. This task introduces transmission delay T^{tx} . Then, the received data should be transmitted to an execution server. Execution servers may be placed at any node in the network, i.e., ranging from the base station itself to a distant node in the core network. The data transmission through the transport network adds the propagation delay T^{prop} to the offloading process. Finally, the received data is processed at the execution server with delay T^{exe} and then is transmitted back to the associated user over the downlink. Therefore, the overall task offloading latency is equal to the summation of all the above mentioned delays in both the uplink and the downlink directions.

B. Motivation

Recently, task offloading has been a subject of extensive research. However, the works in the

literature assessed the impacting factors in a narrow perspective that comes by making some restrictive and unrealistic assumptions [4]–[8]. For example, some works [5]–[7] ignore the impact of radio resource allocation in the process of task offloading while others [4], [8] assume a given feasible set of offloading requests, leaving the admission control problem open. Therefore, there is a need to analyze the task offloading problem in a comprehensive framework. In light of such research, one can identify the impacting factors and their extent on the performance of task offloading.

C. Contributions

In this work, we aim at providing a comprehensive framework for assessing the performance of the task offloading that enables a user to offload a task to any NFV-enabled node in the network rather than offloading to a specific MEC-enabled node (e.g., an edge node). We also consider the impact of radio resource allocation on the task offloading by incorporating a power allocation scheme. Moreover, we assume that each offloaded task should be executed under a maximum tolerable latency constraint that may make the problem of task offloading infeasible. Therefore, we further consider an admission control mechanism to avoid such infeasibility.

In this paper, we assume that a task is offloaded to an NFV-enabled node for execution and then the processed data of that task is forwarded through a network of NFV-enabled nodes towards a radio access network with centralized radio access network (C-RAN) architecture. The data is then transmitted to the intended user through a wireless link.

The main properties of our proposed framework are as follows:

- **Task offloading to multiple NFV-enabled MEC nodes:** When MEC meets NFV, it is possible to offload various types of tasks to any node in the network rather than a predetermined node (e.g., an MEC server at the edge node). As a result, we open the possibility of offloading a requested task to any NFV-enabled node in the network as long as the task maximum tolerable latency is satisfied. The NFV-enabled nodes can be located either at the edge of the radio network or at a large distance from the radio network.
- **Joint power allocation and task offloading (JPATO):** We consider joint radio transmission power allocation and task offloading in a C-RAN architecture. In the optimization problem, we consider to jointly: a) allocate radio transmission power, b) determine the hosting NFV-enabled nodes, and c) allocate computational resources. With a joint optimization, weak radio channel conditions can be compensated by a proper task offloading decision, and

conversely, limited computational resources can be compensated by consuming more radio transmission power. As a result, more requested tasks can be accepted compared to a disjoint optimization where radio transmission power allocation and task offloading decisions are independently performed.

- **Offloading decision and computational resource allocation:** In a MEC-enabled network, a user chooses to whether offload its associated task or locally execute the task. Furthermore, when there are multiple MEC servers in the network, the user determines the optimal MEC server. On the other hand, the computational resource allocation in the user's device and/or MEC server is provided by the underlying framework. Our proposed framework determines both offloading decisions and the allocation of computational resources.
- **Latency modeling:** We model end-to-end (E2E) latency of tasks as the summation of radio transmission, propagation through the network of NFV-enabled nodes, and processing delays. We further assume that each task should be served under a maximum tolerable E2E latency constraint. Due to limited computational and radio resources, this assumption may make the optimization problem infeasible. Therefore, an admission control mechanism is needed.
- **Admission control:** As serving of all the incoming requests may not be feasible, we adopt an admission control mechanism, whose aim is to find the maximum cardinality subset of tasks that can be served by available resources in the network. In doing so, we propose to elasticize the constraints of the optimization problem by a set of non-negative auxiliary variables which we refer to as *elastic variables*. The elastic variables take the zero value for a feasible problem and take positive values for an infeasible optimization problem. Thus, we eliminate the tasks with associated positive elastic variable one by one, until a subset of feasible tasks is obtained.
- **Solution:** Since both JPATO and the admission control optimization problems are non-convex, we adopt an alternate search method (ASM) to find a sub-optimal solution by solving optimization subproblems with respect to each optimization variable. The subproblem of computational resource allocation is convex. We adopt the convex-concave procedure (CCP) to overcome the non-convexity of the power allocation subproblem. The offloading decision subproblem is reformulated as an integer linear programming (ILP). Eventually, we propose a new heuristic algorithm in order to improve the performance of ASM in the proposed admission control algorithm.

- **Disjoint optimization:** We further provide a disjoint algorithm for radio transmission power allocation and task offloading as the baseline of comparison. In doing so, we decouple the maximum tolerable E2E latency of tasks into two parts: radio transmission and task offloading. We first consider the subproblem of radio transmission power allocation under its latency constraint. Then, the task offloading subproblem is solved under its associated latency constraint. We also leverage the admission control mechanism to ensure the feasibility of each subproblem.
- **Lower bound on optimal solution:** To evaluate the efficiency of JPATO, we find a lower bound on the optimal solution of the optimization problem. In this way, we make some relaxations that provide a lower bound on the optimal solution. We find the optimal power allocation by leveraging the benefits of large-scale antenna arrays. Then, by performing an exhaustive search over all possible task offloading decisions and utilizing Karush–Kuhn–Tucker (KKT) optimality conditions, we find the optimal solution for each set of offloading decisions. Then, we find the optimal offloading decision set which results in the lowest objective value. As shown by simulations, the lower bound is tight and is attainable by JPATO.
- **Convergence:** The convergence of both admission control and JPATO optimization algorithms is proved by showing that the value of the objective function is non-increasing in each iteration.
- **Complexity:** We analyze the computational complexity of the proposed algorithms including the interior-point method (IPM) and the proposed heuristic algorithm.

D. Organization

The rest of this paper is organized as follows. Section II summarizes the related works in the task offloading literature. Section III introduces the system model. Section IV describes the optimization problem formulation. In Section V, we propose JPATO algorithm as well as the admission control mechanism, while the disjoint power allocation and task offloading (DPATO) algorithm is proposed in Section A. The optimal resource allocation is obtained in Section B. The computational complexity analysis of the proposed methods is provided in Section V-E. The simulation results are presented in Section VI. Finally, we conclude the paper in Section VII.

E. Notation

The notation used in this paper are given as follows. The vectors are denoted by bold lowercase symbols. Operators $\|\cdot\|$ and $|\cdot|$ are vector norm and absolute value of a scalar, respectively. $(\mathbf{a})^T$ stands for transpose of \mathbf{a} and $[a]^+ = \max(a, 0)$. $\mathcal{A} \setminus \{a\}$ discards the element a from the set \mathcal{A} . Finally, $\mathbf{a} \sim \mathcal{CN}(\mathbf{0}, \Sigma)$ is a complex Gaussian vector with zero mean and covariance matrix Σ .

II. RELATED WORKS

In this section, we classify the related works into four categories and show their limitations compared with our proposed framework. The categories include:

1) **Task offloading to multiple NFV-enabled MEC nodes:** The main objective of task offloading architectures is to offload a task to a single MEC server to select a MEC node out of multiple ones. Specifically, [6], [9] consider offloading a task to a set of MEC servers in a multi-tier heterogeneous network while [7], [10], [11] propose to offload a user's task to one of MEC servers at base stations in a multi-cell network. Interestingly, the MEC servers are located in the radio access network. Therefore, the computational resources in other parts of the network are intentionally not considered. Eventually, the offloading procedure of a user's task to multiple NFV-enabled nodes is proposed in [4]. However, [4] does not include radio resource allocation. In contrast to these works, our proposed framework facilitates offloading a task to any NFV-enabled node in the network, while radio resources are allocated as well.

2) **Offloading decision and resource allocation:** The task offloading is mainly comprised of two steps, namely: i) the offloading decision to select the node executing the task, and ii) the resource allocation that determines the allocated resources for task execution in order to fulfill a given objective. In this context, different works only focus on offloading decision with given radio and computational resources for each task [4]–[7], [9], [12], [13], while others include resource allocation as well [10], [14]–[22]. Our proposed framework includes both task offloading decision and resource allocation. In addition, the resource allocation includes both radio and computational resource allocation.

3) **Joint Radio and Computational Resource Allocation:** Extensive research is made on joint radio and computational resource allocation [8], [10], [13]–[27]. In these works, radio resources including transmission power and/or bandwidth are allocated together with computational resources to execute a task. In general, the objective is to execute a task with minimum consumed

energy [13], [14], [18], [20], [22], [24], [26], [27]. On the other hand, minimizing a weighted combination of consumed energy and latency is performed in [8], [10], [15]–[17], [21], [25]. Moreover, the impact of radio channels on the task offloading without radio resource allocation is faced by [7], [9], [11], [12], [28], [29]. In these works, the latency of data transmission over radio channels is taken into account, thus affecting the optimal offloading decision. However, the radio resources are not allocated for offloading decision optimization. Note that in these joint radio and computational resource allocations, only computational resources in the access network (i.e., edge nodes) are utilized. In contrast to such previous works, our proposed method considers the computational resources in all NFV-enabled nodes (i.e., both edge nodes and distant nodes). Moreover, the objective of our framework is to minimize the consumed energy while satisfying maximum tolerable latency of tasks.

4) *Admission Control Mechanisms*: Different works falling under this category assume sufficient available resources [4], [8] for serving the requested tasks. In other frameworks, a task is only offloaded when it is beneficial, i.e., a task offloading decision is chosen when it leads to minimum energy or latency [12]. However, in general, when the requested tasks are under a maximum tolerable latency constraint, a problem infeasibility may be introduced due to the limited amount of available resources. Therefore, an admission control mechanism is needed to decide whether a task is accepted or rejected. The decision about accepting a task is mainly made by typically solving an integer optimization problem, which is in general very challenging to be solved [5], [6], [10], [14], [16], [20]–[22], [27]. As a result, in this work we propose heuristic methods for admission control mechanisms. In our framework, we aim to find a subset of requested tasks with maximum cardinality. In doing so, we incorporate real-valued positive optimization variables to generate a linear programming problem that can be easily solved with a reasonable complexity.

III. SYSTEM MODEL

The structure of the radio access network including channel model and signaling scheme are described in this section. In addition, the NFV-enabled network including network graph, computational capacity, and bandwidth of network links are modeled.

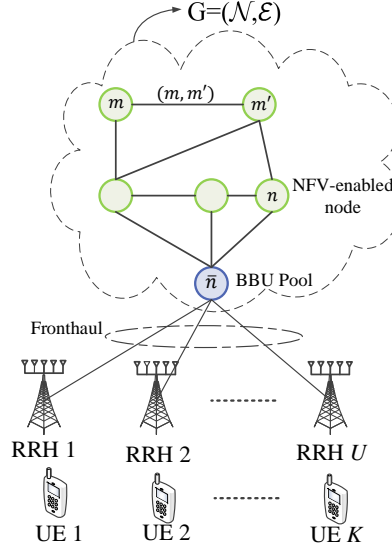


Fig. 2: System model.

A. Radio Access Network

We consider a C-RAN architecture with a baseband unit (BBU) pool which serves a set of U radio remote heads (RRHs). Each RRH is equipped with M antennas. The set of all users is denoted by \mathcal{K} . The total number of users is $K = |\mathcal{K}|$, each of which is equipped with a single antenna. The considered model is shown in Fig. 2. It is assumed that each RRH is connected to the BBU pool through a fronthaul link.

We assume that each user requests a single task. Each UE task k is represented by a triplet $\phi_k = \langle L_k, D_k, T_k \rangle$, where L_k is the load of task k (i.e., the required CPU cycles), D_k is the data size of task k (in terms of bits), and T_k is the maximum tolerable latency of task k .

Each user transmits the data of the corresponding task to its serving RRH through a wireless link in the uplink direction. We assume that each user is served by a single RRH. The set of users served by RRH u is $\mathcal{K}_u = \{k \in \mathcal{K} | J_u^k = 1\}$ where J_u^k is an indicator which equals 1 if user k is connected to RRH u (0 otherwise). In this paper, we assume that the user-RRH assignment is given and fixed. Focusing on the wireless link, we assume a narrow-band block fading channel model [22]. The channel vector between user k and RRH u is denoted by $\mathbf{h}_{u,k}$, where $\mathbf{h}_{u,k} = \sqrt{Q_{u,k}} \tilde{\mathbf{h}}_{u,k}$ in which $Q_{u,k}$ represents the path loss between RRH u and UE k and small-scale fading is modeled as $\tilde{\mathbf{h}}_{u,k} \sim \mathcal{CN}(\mathbf{0}, \mathbf{I}_M)$. Similar to [17], [18], we assume the channel state information is constant over the offloading time duration. As we show through simulations, this assumption is non-restrictive in practical scenarios in sub-6 GHz bands. The

user k transmits a symbol $x_k \sim \mathcal{CN}(\mathbf{0}, 1)$ with transmit power ρ_k toward its serving RRH. The transmit power of each user is constrained to a maximum value, i.e., $\rho_k \leq P_k^{\max} \quad \forall k$. The following signal vector is received at the u^{th} RRH:

$$\mathbf{y}_u = \sum_{k \in \mathcal{K}} \mathbf{h}_{u,k} \sqrt{\rho_k} x_k, \quad \forall u, \quad (1)$$

and is processed with the maximum ratio combining method. The combined signal is given by:

$$\mathbf{z}_u = \mathbf{F}_u^H \mathbf{y}_u, \quad \forall u, \quad (2)$$

where $\mathbf{F}_u = [\mathbf{f}_k], \forall k \in \mathcal{K}_u$ and $\mathbf{f}_k = \frac{\mathbf{h}_{u,k}}{\|\mathbf{h}_{u,k}\|}$. Therefore, the decision signal of user k is given by:

$$z_k = \mathbf{f}_k^H \mathbf{h}_{u,k} \sqrt{\rho_k} x_k + \sum_{j \in \mathcal{K} \setminus \{k\}} \mathbf{f}_k^H \mathbf{h}_{u,j} \sqrt{\rho_j} x_j + \mathbf{f}_k^H \mathbf{n}_u, \quad \forall k \in \mathcal{K}_u,$$

where $\mathbf{n}_u \sim \mathcal{CN}(\mathbf{0}, \sigma_n^2 \mathbf{I}_M)$ is the received noise vector at the u^{th} RRH. Thus, the signal to interference plus noise ratio (SINR) of user k can be written as:

$$\text{SINR}_k = \frac{\|\mathbf{h}_{u,k}\|^2 \rho_k}{\sum_{j \in \mathcal{K} \setminus \{k\}} \frac{|\mathbf{h}_{u,k}^H \mathbf{h}_{u,j}|^2}{\|\mathbf{h}_{u,k}\|^2} \rho_j + \sigma_n^2}, \quad \forall k \in \mathcal{K}_u. \quad (3)$$

Hence, the achievable data rate for user k is $R_k = W \log_2(1 + \text{SINR}_k)^1$ bits per second (bps), where W is the radio access network bandwidth. Therefore, the incurred delay related to task k 's data transmission of the uplink is given by $T_k^{\text{tx}} = \frac{D_k}{R_k}$. Finally, the sum of data rates served by RRH u should be less than the bandwidth of fronthaul links, i.e., $\sum_{k \in \mathcal{K}_u} R_k \leq B_{f,u}, \forall u$.

In this paper, similar to [29], [12], [13], we assume the output data size of task k after the execution is small. Moreover, since the power budget in downlink direction is generally large, the transmission delay of downlink can be assumed negligible and therefore, our focus in the radio access network is solely on the uplink.

B. NFV-enabled Network

The NFV-enabled nodes are interconnected through a network $G = (\mathcal{N}, \mathcal{E})$ where \mathcal{N} and \mathcal{E} are the set of nodes and links connecting the nodes, respectively. A typical node in \mathcal{N} is denoted by n while the BBU pool is indicated by \bar{n} (which also is a node in \mathcal{N}). Moreover, the link

¹For wide-band channel model, the data rate of user k is determined by the sum rate of all sub-carriers allocated to user k .

²It should be noted that no buffering is assumed in the transport network switching. Therefore, there is no need for transmission time of tasks traffic associated with the network graph links to be taken into account.

between two nodes m and m' is denoted by (m, m') . The nodes and links of the network can provide a limited amount of resources. The processing capacity (i.e., the maximum CPU cycles per second that could be carried out) of NFV-enabled node n is indicated by Υ_n . Moreover, the bandwidth of link (m, m') is indicated by $B_{(m, m')}$ in terms of bps.

A task offloading decision consists of specifying the placement of each task at node n and its associated path from \bar{n} to n . We denote the b^{th} path between nodes \bar{n} and n as p_n^b where $b \in \mathcal{B}_n = \{1 \cdots B_n\}$ and B_n is the total number of paths between nodes \bar{n} and n . In order to choose a node and its associated path, we define the decision variable $\xi_{p_n^b}^k$ which equals 1 when the task ϕ_k is placed at node n and sent over path p_n^b and equals 0 otherwise. To ensure that a task is offloaded to one and only one node and path, we introduce the following constraint:

$$\sum_{n \in \mathcal{N}} \sum_{b \in \mathcal{B}_n} \xi_{p_n^b}^k = 1, \quad \forall k. \quad (4)$$

To determine whether a link contributes to a path, the indicator $I_{p_n^b}^{(m, m')}$ is defined, which is equal to 1 when link (m, m') contributes to path p_n^b (0 otherwise). Moreover, the set of all links that contribute to a path can be defined as: $\mathcal{E}_{p_n^b} = \{(m, m') \in \mathcal{E} | I_{p_n^b}^{(m, m')} = 1\}$. The amount of computational resources allocated to task k is denoted by v_k (in terms of CPU cycles per second). We assume that the execution of tasks are fully performed at only one node (i.e., full offloading). To ensure that the allocated computational resources do not violate the processing capacity of that node, we should have:

$$\sum_{k \in \mathcal{K}} \sum_{b \in \mathcal{B}_n} v_k \xi_{p_n^b}^k \leq \Upsilon_n, \quad \forall n. \quad (5)$$

Since the data of task k is sent over the network with rate R_k , the aggregated rates of all tasks that pass a link should not exceed its bandwidth. This can be ensured by the following constraint:

$$\sum_{k \in \mathcal{K}} \sum_{n \in \mathcal{N}} \sum_{b \in \mathcal{B}_n} I_{p_n^b}^{(m, m')} \xi_{p_n^b}^k R_k \leq B_{(m, m')}, \quad \forall (m, m') \in \mathcal{E}. \quad (6)$$

The incurred delay caused by execution of task k is $T_k^{\text{exe}} = \frac{L_k}{v_k}$. The data of task k is sent to NFV-enabled node n over the uplink for execution. After the execution of the task, it should be sent toward the BBU pool (i.e., node \bar{n}) over the downlink. In this paper, we assume the path of uplink and downlink are the same. Therefore, the overall propagation delay of task k over the path p_n^b is twice the propagation delay of path p_n^b . Thus, the propagation delay of task k is given by $T_k^{\text{prop}} = 2 \sum_{n \in \mathcal{N}} \sum_{b \in \mathcal{B}_n} \sum_{(m, m') \in \mathcal{E}_{p_n^b}} \xi_{p_n^b}^k \delta_{(m, m')}$, where $\delta_{(m, m')}$ is the propagation

delay of link (m, m') . We assume that the bandwidth consumption of links imposes a specific cost to operators, thus we need to calculate the overall traffic of users that pass through links and determine the cost of passing this traffic. The overall cost of bandwidth consumption is calculated as $\beta = \sum_{k=1}^K \sum_{n \in \mathcal{N}} \sum_{b \in \mathcal{B}_n} \sum_{(m, m') \in \mathcal{E}_{p_n^b}} \xi_{p_n^b}^k \gamma_{(m, m')} R_k$, where $\gamma_{(m, m')}$ determines the cost of transmitting 1 bps traffic on link (m, m') . Table I summarizes the notation used in the paper.

TABLE I: Main Notation.

Notation	Definition	Notation	Definition
U, M, K	Number of RRHs, antennas and users	W	Radio access network bandwidth
$\mathcal{K}, \mathcal{N}, \mathcal{E}$	Set of all users, nodes and links	\mathcal{K}_u	Set of users served by RRH u
ϕ_k	Task of UE k	$\mathbf{h}_{u, k}$	Channel vector between user k and RRH u
L_k, D_k, T_k	Load, data size and maximum tolerable latency of task k	$\xi_{p_n^b}^k$	Decision variable for assignment of node n and its associated path p_n^b to task ϕ_k
Υ_n	Processing capacity of node n	$B_{f, u}$	Bandwidth of fronthaul link for RRH u
$B_{(m, m')}, \delta_{(m, m')}$	Bandwidth and propagation delay of link (m, m')	Λ_n	Computational energy efficiency coefficient of the node n
$\gamma_{(m, m')}$	Cost of forwarding traffic on (m, m')	P_k^{\max}	Power budget of user k
p_n^b	b^{th} path between nodes \bar{n} and n	v_k	Computational resources allocated to task ϕ_k
\mathcal{B}_n	Set of paths between nodes \bar{n} and n	ρ_k	Allocated transmission power to user k
$\mathcal{E}_{p_n^b}$	Set of all links that contribute in the path p_n^b	α_k	Elasticization variable of task ϕ_k
$I_{p_n^b}^{(m, m')}$	Indicator determining whether link (m, m') contributes in path p_n^b	R_k	Data rate of task k
J_u^k	Indicator determining whether user k is assigned to RRH u	T_k^{exe}	Execution delay of task k
T_k^{tx}	Radio transmission delay of task k	T_k^{PROP}	Propagation delay of task k
β	Cost of bandwidth consumption		

IV. PROBLEM FORMULATION

In this section, we formulate JPATO problem. The overall objective is to offload and execute the tasks with acceptable E2E latency in a cost-efficient fashion. The overall cost of task offloading includes: 1) the radio transmission cost, which includes the power consumption of all RRHs, 2) the forwarding cost associated with the traffic injected in the network, and 3) the cost of consumed power of NFV-enabled nodes. Hence, the overall cost function can be stated as $\Psi(\boldsymbol{\xi}, \mathbf{v}, \boldsymbol{\rho}) = \beta + \zeta \sum_{k \in \mathcal{K}} \rho_k + \eta \sum_{n \in \mathcal{N}} \sum_{k \in \mathcal{K}} \sum_{b \in \mathcal{B}_n} \Lambda_n \xi_{p_n^b}^k v_k^3$, where $\boldsymbol{\xi} = [\xi_{p_1^1}, \dots, \xi_{p_N^K}]^T$, $\mathbf{v} = [v_1, \dots, v_K]^T$, and $\boldsymbol{\rho} = [\rho_1, \dots, \rho_K]^T$ are the vectors of all $\xi_{p_n^b}^k$, v_k , and ρ_k , respectively, and Λ_n denotes the computational energy efficiency coefficient of node n [19]. Moreover, ζ and η are weight factors.

Therefore, the joint power allocation and task offloading optimization problem can be written as:

$$\begin{aligned}
& \min_{\xi, \mathbf{v}, \boldsymbol{\rho}} \Psi(\boldsymbol{\xi}, \mathbf{v}, \boldsymbol{\rho}) \\
& \text{s.t.} \quad \text{C1: } T_k^{\text{exe}} + T_k^{\text{prop}} + T_k^{\text{tx}} \leq T_k, \quad \forall k, \\
& \quad \quad \text{C2: } \sum_{k \in \mathcal{K}} \sum_{b \in \mathcal{B}_n} v_k \xi_{p_n^b}^k \leq \Upsilon_n, \quad \forall n, \\
& \quad \quad \text{C3: } \sum_{k \in \mathcal{K}} \sum_{n \in \mathcal{N}} \sum_{b \in \mathcal{B}_n} I_{p_n^b}^{(m, m')} \xi_{p_n^b}^k R_k \leq B_{(m, m')}, \quad \forall (m, m') \in \mathcal{E}, \\
& \quad \quad \text{C4: } \sum_{k \in \mathcal{K}_u} R_k \leq B_{f, u}, \quad \forall u, \\
& \quad \quad \text{C5: } \rho_k \leq P_k^{\text{max}}, \quad \forall k, \\
& \quad \quad \text{C6: } \sum_{n \in \mathcal{N}} \sum_{b \in \mathcal{B}_n} \xi_{p_n^b}^k = 1, \quad \forall k,
\end{aligned} \tag{7}$$

under variables: $\boldsymbol{\xi} \in \{0, 1\}$, $\mathbf{v} \geq 0$, $\boldsymbol{\rho} \geq 0$. Constraint C1 guarantees that the maximum tolerable latency of task offloading is respected. Constraints C2 and C3 make sure that all tasks are offloaded without violation in computational capacity of nodes as well as bandwidth of links, respectively. Constraint C4 ensures the maximum capacity of fronthaul links. Constraint C5 ensures the power budget of users while constraint C6 ensures that each task is offloaded at only one node and traversing only one path.

V. JOINT POWER ALLOCATION AND TASK OFFLOADING (JPATO)

In this section, we propose a solution for optimization problem (7). This problem is highly non-convex due to the integer variable $\boldsymbol{\xi}$ as well as non-convexity of C1-C4. Therefore, we adopt an approach based on ASM to divide the main problem into multiple subproblems, each of them associated to a proper subset of the optimization variable. Then, each set of variables is optimized given the values of other sets of variables and a sub-optimal solution can be obtained by the proposed iterative solution algorithm. The proposed ASM needs a feasible initialization. It is likely for constraint C1 to make the main problem infeasible. Thus, we need to propose an admission control mechanism to find the tasks that cause infeasibility. In the following, we exclude such tasks and we seek for the optimal solution of joint resource allocation problem for the remaining ones.

A. Admission Control

To find the tasks which cause infeasibility, we use the elasticization approach of [30]. In particular, the constraints are elasticized by introducing elastic variables that extend the bounds

on constraints. More formally, an infeasible set of constraints $f_k(x) \leq 0$, $k = 1, \dots, K$ can be elasticized by non-negative elastic variables α_k as $f_k(x) - \alpha_k \leq 0$. A feasibility problem is then constructed by replacing the original objective function with the sum of elastic variables, i.e., $\sum_{k=1}^K \alpha_k$, subject to elasticized constraints. By solving the feasibility problem, the constraints which cause infeasibility can be found by determining the constraints with positive associated elastic variables. The feasibility problem of (7) w.r.t. the optimization variables ξ, \mathbf{v}, ρ , and α can be written as:

$$\begin{aligned} & \min_{\xi, \mathbf{v}, \rho, \alpha} \quad \sum_{k \in \mathcal{K}} \alpha_k \\ & \text{s.t.} \quad \text{C1-a: } T_k^{\text{exe}} + T_k^{\text{prop}} + T_k^{\text{tx}} - \alpha_k \leq T_k, \quad \forall k \in \mathcal{K} \\ & \quad \quad \text{C2-C6,} \end{aligned} \quad (8)$$

under variables: $\xi \in \{0, 1\}$, $\mathbf{v} \geq 0$, $\rho \geq 0$, $\alpha \geq 0$. Note that only C1 of (8) is elasticized because by elimination of C1, the optimization problem (7) is always feasible. Thus, we seek for the tasks whose maximum tolerable latency is violated and eliminate them one by one until a feasible set of tasks remains. The solution of (8) not only provides the infeasible constraints but also determines the level of infeasibility, i.e., constraints with larger associated elastic variable need more resources to become feasible. Therefore, we start by eliminating of tasks with larger values of elastic variables.

Without loss of equivalence, we can add the summation of inequalities in C1-a as a new constraint (C7) to optimization problem (8). Therefore, the optimization problem (8) can be restated as:

$$\begin{aligned} & \min_{\xi, \mathbf{v}, \rho, \alpha} \quad \sum_{k \in \mathcal{K}} \alpha_k \\ & \text{s.t.} \quad \text{C1-a: } T_k^{\text{exe}} + T_k^{\text{prop}} + T_k^{\text{tx}} - \alpha_k \leq T_k, \quad \forall k \\ & \quad \quad \text{C2-C6,} \\ & \quad \quad \text{C7: } \sum_{k \in \mathcal{K}} (T_k^{\text{exe}} + T_k^{\text{prop}} + T_k^{\text{tx}} - T_k) \leq \sum_{k \in \mathcal{K}} \alpha_k. \end{aligned} \quad (9)$$

This optimization problem is equivalent of:

$$\begin{aligned} & \min_{\xi, \mathbf{v}, \rho, \alpha} \quad \sum_{k \in \mathcal{K}} (T_k^{\text{exe}} + T_k^{\text{prop}} + T_k^{\text{tx}}) \\ & \text{s.t.} \quad \text{C1-a, C2-C6,} \end{aligned} \quad (10)$$

in which the term $\sum_{k \in \mathcal{K}} T_k$ is removed from the objective due to its constant value. Given a random but feasible set of values for the discrete variable ξ , a feasible computational resource allocation \mathbf{v} , and a feasible power allocation complying with constraints C3 - C6, we find elastic variables given by $\alpha_k = [T_k^{\text{exe}} + T_k^{\text{prop}} + T_k^{\text{tx}} - T_k]^+$. Hence, the elastic variables make

the constraint C1-a active, i.e., C1-a is satisfied with equality. For solving (10), we begin with power allocation, i.e., solving (10) for $\rho \geq 0$, having the other variables fixed. The associated optimization problem is:

$$\begin{aligned} \min_{\rho} \quad & \sum_{k=1}^K T_k^{\text{tx}} \\ \text{s.t.} \quad & \text{C1-a, C3-C5.} \end{aligned} \quad (11)$$

To get rid of highly non-convex objective function of (11), we substitute the objective function with a constant value, e.g., zero. In other words, we find a feasible solution for ρ . Note that this substitution does not impact the performance of admission control, because the constraint C1-a is active and any feasible power allocation results in lower value of T_k^{tx} . Based on above assumptions, we replace (11) with:

$$\begin{aligned} \min_{\rho} \quad & 0 \\ \text{s.t.} \quad & \text{C1-a, C3-C5.} \end{aligned} \quad (12)$$

In solving (12), we note that the constraints C1-a, C3 and C4 are non-convex. Therefore, we need to find a convexified version of this problem. We use the well-known convex-concave procedure (CCP) [31] to convexify (12). In doing so, we first reformulate C1-a as $T_k^{\text{exe},i} + T_k^{\text{prop},i} + \frac{D_k}{R_k} - \alpha_k \leq T_k$, where $T_k^{\text{exe},i}$ and $T_k^{\text{prop},i}$ are the execution time and propagation time of task k obtained from the results of the subproblems associated with variables \mathbf{v} and $\boldsymbol{\xi}$ at i^{th} iteration, respectively. Hence, it holds that:

$$R_k \geq \frac{D_k}{T_k + \alpha_k - T_k^{\text{prop},i} - T_k^{\text{exe},i}}. \quad (13)$$

In order to convexify (13), we need a concave approximation of R_k with respect to ρ . The rate R_k can be written as:

$$R_k = W \log_2 \left(\frac{\sum_{j \in \mathcal{K}} \frac{|\mathbf{h}_{u,k}^H \mathbf{h}_{u,j}|^2}{|\mathbf{h}_{u,j}|^2} \rho_j + \sigma^2}{\sum_{j \in \mathcal{K} \setminus \{k\}} \frac{|\mathbf{h}_{u,k}^H \mathbf{h}_{u,j}|^2}{|\mathbf{h}_{u,j}|^2} \rho_j + \sigma^2} \right), \quad k \in \mathcal{K}_u, \quad (14)$$

which is equivalent to:

$$R_k = \underbrace{W \log_2 \left(\sum_{u=1}^U \sum_{j \in \mathcal{K}_u} \frac{|\mathbf{h}_{u,k}^H \mathbf{h}_{u,j}|^2}{|\mathbf{h}_{u,j}|^2} \rho_j + \sigma^2 \right)}_{h_k(\boldsymbol{\rho})} - \underbrace{W \log_2 \left(\sum_{u=1}^U \sum_{j \in \mathcal{K}_u \setminus \{k\}} \frac{|\mathbf{h}_{u,k}^H \mathbf{h}_{u,j}|^2}{|\mathbf{h}_{u,j}|^2} \rho_j + \sigma^2 \right)}_{g_k(\boldsymbol{\rho})}. \quad (15)$$

Based on CCP, since both $h_k(\boldsymbol{\rho})$ and $g_k(\boldsymbol{\rho})$ are concave functions of $\boldsymbol{\rho}$, we need to find a linear approximation of $g_k(\boldsymbol{\rho})$. The linear approximation of R_k can be given as $\hat{g}_k(\boldsymbol{\rho}) = g_k(\boldsymbol{\rho}^0) + \nabla g_k(\boldsymbol{\rho}^0)^T(\boldsymbol{\rho} - \boldsymbol{\rho}^0)$ where:

$$[\nabla g_k(\boldsymbol{\rho})]_i = \begin{cases} \frac{W \sum_{u=1}^U I_u^i \frac{|\mathbf{h}_{u,k}^H \mathbf{h}_{u,i}|^2}{|\mathbf{h}_{u,i}|^2}}{\ln(2) \left(\sum_{u=1}^U \sum_{j \in \mathcal{K}_u \setminus \{k\}} \frac{|\mathbf{h}_{u,k}^H \mathbf{h}_{u,j}|^2}{|\mathbf{h}_{u,j}|^2} \rho_j + \sigma^2 \right)}, & i \in \mathcal{K} \setminus \{k\}, \\ 0, & i = k. \end{cases} \quad (16)$$

Next, we focus on the convex approximation of constraints C3 and C4. To this aim, we find a convex approximation of R_k . Based on CCP, $h_k(\boldsymbol{\rho})$ is approximated by a linear function. Thus, we have $\hat{h}_k(\boldsymbol{\rho}) = h_k(\boldsymbol{\rho}^0) + \nabla h_k(\boldsymbol{\rho}^0)^T(\boldsymbol{\rho} - \boldsymbol{\rho}^0)$, where:

$$[\nabla h_k(\boldsymbol{\rho})]_i = \frac{W \sum_{u=1}^U I_u^i \frac{|\mathbf{h}_{u,k}^H \mathbf{h}_{u,i}|^2}{|\mathbf{h}_{u,i}|^2}}{\ln(2) \left(\sum_{u=1}^U \sum_{j \in \mathcal{K}_u} \frac{|\mathbf{h}_{u,k}^H \mathbf{h}_{u,j}|^2}{|\mathbf{h}_{u,j}|^2} \rho_j + \sigma^2 \right)}, \quad i \in \mathcal{K}, \quad (17)$$

The convexified version of subproblem (11) can be stated as:

$$\begin{aligned} & \min_{\boldsymbol{\rho}} \quad 0 \\ & \text{s.t.} \quad \text{C1-b} \quad h_k(\boldsymbol{\rho}) - \hat{g}_k(\boldsymbol{\rho}) \geq \frac{D_k}{T_k + \alpha_k - T_k^{\text{prop},i} - T_k^{\text{exe},i}}, \quad \forall k \in \mathcal{K} \\ & \quad \text{C3-a:} \quad \sum_{k \in \mathcal{K}} \sum_{n \in \mathcal{N}} \sum_{b \in \mathcal{B}_n} I_{p_n^b}^{(m,m')} \xi_{p_n^b}^k \left(\hat{h}_k(\boldsymbol{\rho}) - g_k(\boldsymbol{\rho}) \right) \leq B_{(m,m')}, \quad \forall (m, m') \in \mathcal{E} \\ & \quad \text{C4-a:} \quad \sum_{k \in \mathcal{K}_u} \left(\hat{h}_k(\boldsymbol{\rho}) - g_k(\boldsymbol{\rho}) \right) \leq B_{f,u}, \quad \forall u \\ & \quad \text{C5:} \quad \rho_k \leq P_k^{\max}, \quad \forall k, \end{aligned} \quad (18)$$

under variable: $\boldsymbol{\rho} \geq 0$. Based on CCP in Algorithm 1 and starting from a feasible $\boldsymbol{\rho}^0$, an iterative solution of (18) provides a sub-optimal solution of (12). Note that any feasible solution of (18) is also feasible in (12) [31].

Algorithm 1: Convex-concave procedure for solving (11).

Input: Feasible $\boldsymbol{\rho}^0$, $i = 0$, $\epsilon = 10^{-3}$, $I_{\max}^\rho = 10^3$

1 repeat

% Allocate power to users

2 Solve (18) and set $\boldsymbol{\rho}^{i+1} = \boldsymbol{\rho}^*$

3 $i = i + 1$

4 until $\sum_{k \in \mathcal{K}} \hat{T}_k^{\text{tx}}(\boldsymbol{\rho}^i) - \sum_{k \in \mathcal{K}} \hat{T}_k^{\text{tx}}(\boldsymbol{\rho}^{i-1}) \leq \epsilon$ or $i \geq I_{\max}^\rho$

Output: $\boldsymbol{\rho}^*$

The optimization problem associated with $\mathbf{v} \geq 0$ is:

$$\begin{aligned} \min_{\mathbf{v}} \quad & \sum_{k \in \mathcal{K}} T_k^{\text{exe}} \\ \text{s.t.} \quad & \text{C1-a, C2.} \end{aligned} \quad (19)$$

Since the function $\frac{L_k}{v_k}$ is convex over $v_k > 0$, the subproblem (19) is convex and can be efficiently solved using Interior Point Method (IPM). Given the solution of subproblems (18) and (19), we find the binary decision variable ξ . The associated subproblem is:

$$\begin{aligned} \min_{\xi} \quad & \sum_{k \in \mathcal{K}} T_k^{\text{prop}} \\ \text{s.t.} \quad & \text{C2, C3, C6.} \end{aligned} \quad (20)$$

This subproblem is an ILP problem that can be efficiently solved by adopting off-the-shelf solvers [32]. Finally, given \mathbf{v} , ρ , and ξ as the solutions of the associated subproblems, the subproblem for finding elastic variable α is given by:

$$\begin{aligned} \min_{\alpha} \quad & \sum_{k \in \mathcal{K}} \alpha_k \\ \text{s.t.} \quad & \text{C1-a,} \end{aligned} \quad (21)$$

which is a linear programming and whose solution is simply can be found as $\alpha_k = [T_k^{\text{exe}} + T_k^{\text{prop}} + T_k^{\text{tx}} - T_k]^+$. Since the objective of (20) is to minimize $\sum_{k \in \mathcal{K}} T_k^{\text{prop}}$, the solver tries to find the nodes with lowest associated propagation delay even if there are unused computational resources that can decrease the value of $\sum_{k \in \mathcal{K}} (T_k^{\text{exe}} + T_k^{\text{prop}})$. To resolve this issue, we consider the optimization problem:

$$\begin{aligned} \min_{\alpha, \mathbf{v}, \xi} \quad & \sum_{k \in \mathcal{K}} \alpha_k \\ \text{s.t.} \quad & \text{C1-C3, C6,} \end{aligned} \quad (22)$$

which can offload the tasks to the nodes that can minimize $T_k^{\text{exe}} + T_k^{\text{prop}}$. In order to solve (22), we propose a novel heuristic method, whose goal is to search among all the nodes that can provide more computational resources to task ϕ_k . As in Algorithm 2, we start from the tasks with the lowest positive values of elastic variable and calculate the amount of unused computational resources at all nodes formally expressed as $\tilde{\Upsilon}_n^k = \Upsilon_n - \sum_{j \in \mathcal{K} \setminus \{k\}} \sum_{b \in \mathcal{B}_n} v_j \xi_{p_n^b}^j$. By assuming $v_k = \tilde{\Upsilon}_n^k$, the value of $T_k^{\text{exe}} + T_k^{\text{prop}}$ is calculated for all nodes whose paths have enough bandwidth. The available bandwidth of link (m, m') can be obtained as $\tilde{B}_{(m, m')}^k = B_{(m, m')} - \sum_{j \in \mathcal{K} \setminus \{k\}} \sum_{n \in \mathcal{N}} \sum_{b \in \mathcal{B}_n} I_{p_n^b}^{(m, m')} \xi_{p_n^b}^j R_j$. Then, having the available resources of nodes and links, the feasible node and path that minimize the value of $T_k^{\text{exe}} + T_k^{\text{prop}}$ are selected. Note that the proposed heuristic finds both the offloading node and the required computational resources

provided by that node. This is in contrast with the conventional routing methods in which the destination node is known in advance. As a result, conventional routing methods can not be utilized in our method. After this step, we calculate the value of $\tilde{\alpha}_k = T_k^{\text{exe}} + T_k^{\text{prop}} + T_k^{\text{tx}} - T_k$. The negativeness of $\tilde{\alpha}_k < 0$ means that task ϕ_k is over-provisioned. Thus, we update v_k such that $\tilde{\alpha}_k = 0$.

Algorithm 2: ASM modification algorithm for solving (22).

Input: α, ξ, v

```

1 sort  $\alpha$ :  $\alpha_{[1]} \leq \alpha_{[2]} \leq \dots \alpha_{[|\mathcal{K}|]}$ 
2 for  $k = [1] : [|\mathcal{K}|]$  do
    % Find a feasible node according to the bandwidth of paths terminating at that node
3    $\mathcal{N}^k = \{n \in \mathcal{N} | \exists b : R_k \leq \tilde{B}_{(m,m')}^k \forall (m, m') \in \mathcal{E}_{p_n^b}\}$ 
4    $\tilde{\Upsilon}_n^k = \Upsilon_n - \sum_{j \in \mathcal{K} \setminus \{k\}} \sum_{b \in \mathcal{B}_n} v_j \xi_{p_n^b}^j, \quad \forall n$ 
    % Find the best node and associated path
5    $(n^*, b^*) = \arg \min_{n \in \mathcal{N}^k, b \in \mathcal{B}_n} T^{\text{exe}}(\tilde{\Upsilon}_n^k) + T^{\text{prop}}(\xi_{p_n^b}^k)$ 
    % Update elastic variables
6    $\tilde{\alpha}_k = T_k^{\text{tx}} + T_k^{\text{exe}}(\tilde{\Upsilon}_{n^*}^k) + T_k^{\text{prop}}(\xi_{p_{n^*}^{b^*}}^k) - T_k$ 
7   if  $\tilde{\alpha}_k < 0$  then
8     set  $v_k = \frac{L_k}{T_k - T_k^{\text{tx}} - T_k^{\text{prop}}}$ , and  $\alpha_k^* = 0$ 
9   else
10     $\alpha_k^* = \tilde{\alpha}_k$ 

```

Output: α^*, ξ^*, v^*

The feasibility problem (8) is solved by alternating solution of (18)-(22). Moreover, we need to reject the tasks that make the joint optimization problem (7) infeasible. According to Algorithm 3, after the accomplishment of Algorithm 2, we find the value of the maximum elastic variable. If the maximum elastic value is positive, the associated task is rejected, the set of the served users is updated, and the feasibility problem is solved for the updated set of the served users. This procedure continues until there is no task with positive associated elastic variable. The output of the admission control algorithm is the set of feasible tasks \mathcal{K}^* as well as the solution of feasibility problem (8), i.e., the values of $\xi^{\text{ini}}, \rho^{\text{ini}}$, and v^{ini} , which are fed into the joint optimization algorithm for solving (7).

Algorithm 3: JPATO admission control algorithm for solving (8).

Input: $\mathcal{K} = \{1, \dots, K\}$, $i = 0$, $\boldsymbol{\rho}^0, \boldsymbol{v}^0$: very small

$\boldsymbol{\xi}^0$: random but compliant with C6, $\boldsymbol{\alpha}^0 = [T_k^{\text{exe}}(\boldsymbol{v}^0) + T_k^{\text{prop}}(\boldsymbol{\xi}^0) + T_k^{\text{tx}}(\boldsymbol{\rho}^0) - T_k]^+$

1 **repeat**

2 **repeat**

 % Allocate power, computational resources, and place the tasks, respectively

 Solve (18) via CCP in Algorithm 1 and set $\boldsymbol{\rho}^{i+1} = \boldsymbol{\rho}^*$

3 Solve (19) and set $\boldsymbol{v}^{i+1} = \boldsymbol{v}^*$

4 Solve (20) and set $\boldsymbol{\xi}^{i+1} = \boldsymbol{\xi}^*$

5 Update \boldsymbol{v}^{i+1} , $\boldsymbol{\xi}^{i+1}$ and $\boldsymbol{\alpha}^{i+1}$ via Algorithm 2

6 $i = i + 1$

7 **until** $\sum_{k \in \mathcal{K}} \alpha_k^{i-1} - \sum_{k \in \mathcal{K}} \alpha_k^i \leq \epsilon$ *or* $i \geq I_{\max}$

 % Eliminate the task with maximum associated elastic variable

8 $k^* = \arg \max_{k \in \mathcal{K}} \alpha_k$

9 **if** $\alpha_{k^*} > 0$ **then**

10 $\mathcal{K} = \mathcal{K} \setminus \{k^*\}$

11 **else**

12 **break**

13 **until** $\sum_{k \in \mathcal{K}} \alpha_k = 0$

Output: $\boldsymbol{\xi}^{\text{ini}}, \boldsymbol{\rho}^{\text{ini}}, \boldsymbol{v}^{\text{ini}}, \mathcal{K}^*$

B. Joint optimization

Given the solution of admission control problem $\boldsymbol{\xi}^{\text{ini}}, \boldsymbol{\rho}^{\text{ini}}, \boldsymbol{v}^{\text{ini}}$, and the set of accepted tasks \mathcal{K} , we seek for the solution of (7). Since the optimization problem (7) and the admission control problem (8) are very similar, the admission control algorithm is applicable to optimization problem with slight modifications. Again, we adopt the ASM for the solution of (7). The subproblems associated with each subset of variables are given in the following. The subproblem for obtaining computational resources is:

$$\begin{aligned} \min_{\boldsymbol{v}} \quad & \sum_{n \in \mathcal{N}} \sum_{k \in \mathcal{K}} \sum_{b \in \mathcal{B}_n} \Lambda_n \xi_{p_n^b}^k v_k^3 \\ \text{s.t.} \quad & \text{C1, C2,} \end{aligned} \tag{23}$$

which is a convex optimization problem. The subproblem of power allocation, after convexification, is given by:

$$\begin{aligned} & \min_{\boldsymbol{\rho}} \quad \sum_{k \in \mathcal{K}} \rho_k \\ & \text{s.t.} \quad \text{C1-c: } h_k(\boldsymbol{\rho}) - \hat{g}_k(\boldsymbol{\rho}) \geq \frac{D_k}{T_k - T_k^{\text{prop},i} - T_k^{\text{exe},i}}, \forall k \in \mathcal{K} \\ & \quad \quad \text{C3-a, C4-a, C5,} \end{aligned} \quad (24)$$

which can be solved using CCP. The task offloading subproblem can be written as:

$$\begin{aligned} & \min_{\boldsymbol{\xi}} \quad \beta_c + \sum_{n \in \mathcal{N}} \sum_{k \in \mathcal{K}} \sum_{b \in \mathcal{B}_n} \Lambda_n \xi_{p_n^b}^k v_k^3 \\ & \text{s.t.} \quad \text{C1-C3, C6.} \end{aligned} \quad (25)$$

which is an ILP. Note that the ASM modification approach is not leveraged for optimization algorithm because there is no motivation for placement of tasks to more distant nodes. This would result in an increase of the forwarding cost and therefore does not affect the computational cost. The optimization algorithm is provided in Algorithm 4.

From the implementation point of view, BBU is responsible for gathering the required information, performing resource allocation, and sending the decisions to the associated entities. Specifically, in JPATO, BBU needs to acquire the channel state information (CSI) of UEs and the available computational resources in the NFV-enabled nodes. CSI of each UE is estimated at its serving RRH and can be forwarded through fronthaul links with negligible latency. In addition, each NFV-enabled node sends the available computational resources to the BBU through network graph. After performing JPATO, BBU transmits the value of allocated powers to RRHs. Next, BBU forwards the received data of tasks as well as the obtained computational resources to associated NFV-enabled nodes based on obtained offloading decision variables. In the downlink, the processed data of tasks are sent to BBU, which in turn transmits UEs processed data to their serving RRH.

C. Convergence analysis

Now, we prove the convergence of the proposed admission control and the joint optimization methods for solving problems (8) and (7), respectively.

Lemma 1. *Algorithm 3 for solving problem (8) converges after sufficient number of iterations.*

Proof. We show that the objective function of (8), i.e., $\sum_{k \in \mathcal{K}} \alpha_k$ is non-increasing in every step of Algorithm 3 and since the objective function is lower bounded by zero, the algorithm converges

Algorithm 4: JPATO optimization algorithm for solving (7) with admitted set of tasks.

Input: $\xi^0 = \xi^{\text{ini}}, \rho^0 = \rho^{\text{ini}}, \mathbf{v}^0 = \mathbf{v}^{\text{ini}}, \mathcal{K}^*, i = 0$

1 repeat

 % Allocate the computational resources, power, and place the tasks, respectively

2 Solve (23) and set $\mathbf{v}^{i+1} = \mathbf{v}^*$

3 Solve (24) via CCP in Algorithm 1 and set $\rho^{i+1} = \rho^*$

4 Solve (25) and set $\xi^{i+1} = \xi^*$

5 $i = i + 1$

6 until $\Psi(\xi^{i-1}, \mathbf{v}^{i-1}, \rho^{i-1}) - \Psi(\xi^i, \mathbf{v}^i, \rho^i) \leq \epsilon$ or $i \geq I_{\text{max}}$

Output: $\xi^*, \rho^*, \mathbf{v}^*$

after sufficient iterations. In i^{th} iteration, the elastic variable α_k is updated as $\alpha_k^i = [T_k^{\text{exe}}(\mathbf{v}^i) + T_k^{\text{prop}}(\xi^i) + T_k^{\text{tx}}(\rho^i) - T_k]^+$. Hence, we need to show the value of each of $\sum_{k \in \mathcal{K}} T_k^{\text{tx}}$, $\sum_{k \in \mathcal{K}} T_k^{\text{exe}}$, and $\sum_{k \in \mathcal{K}} T_k^{\text{prop}}$ is non-increasing in each iteration. In subproblem (11), the constraint C1-a is active, i.e., $T_k^{\text{tx}}(\rho^i) = T_k + \alpha_k - T_k^{\text{exe}}(\mathbf{v}^i) - T_k^{\text{prop}}(\xi^i)$. Therefore, any feasible solution of (18) for ρ^{i+1} results in $T_k^{\text{tx}}(\rho^{i+1}) \leq T_k^{\text{tx}}(\rho^i)$, and hence $\sum_{k \in \mathcal{K}} T_k^{\text{tx}}(\rho^{i+1}) \leq \sum_{k \in \mathcal{K}} T_k^{\text{tx}}(\rho^i)$. Subproblem (19) is convex and obviously we have $\sum_{k \in \mathcal{K}} T_k^{\text{exe}}(\mathbf{v}^{i+1}) \leq \sum_{k \in \mathcal{K}} T_k^{\text{exe}}(\mathbf{v}^i)$. Similarly, (20) is efficiently solved, resulting in $\sum_{k \in \mathcal{K}} T_k^{\text{prop}}(\xi^{i+1}) \leq \sum_{k \in \mathcal{K}} T_k^{\text{prop}}(\xi^i)$. Algorithm 2 finds the node, associated path, and computational resource for task k such that the value of $T_k^{\text{exe}} + T_k^{\text{prop}}$ is minimized. Therefore, in $(i+1)^{\text{th}}$ iteration, Algorithm 2 finds a set of nodes, associated paths, and computational resources such that $\sum_{k \in \mathcal{K}} (T_k^{\text{prop}}(\xi^{i+1}) + T_k^{\text{exe}}(\mathbf{v}^{i+1})) \leq \sum_{k \in \mathcal{K}} (T_k^{\text{prop}}(\xi^i) + T_k^{\text{exe}}(\mathbf{v}^i))$. Based on above, in $(i+1)^{\text{th}}$ iteration, we have $\sum_{k \in \mathcal{K}} (T_k^{\text{exe}}(\mathbf{v}^{i+1}) + T_k^{\text{prop}}(\xi^{i+1}) + T_k^{\text{tx}}(\rho^{i+1}) - T_k) \leq \sum_{k \in \mathcal{K}} (T_k^{\text{exe}}(\mathbf{v}^i) + T_k^{\text{prop}}(\xi^i) + T_k^{\text{tx}}(\rho^i) - T_k)$, which results in $\sum_{k \in \mathcal{K}} \alpha_k^{i+1} \leq \sum_{k \in \mathcal{K}} \alpha_k^i$.

Algorithm 3 may eliminate the constraints associated with the task with maximum elastic variable. This elimination is equivalent to removing the constraints of (8) associated with the eliminated task. Removing some constraints of (8) results in extension of the feasible set of (8) which in turn results in a lower objective value in the next iteration. Thus, the value of $\sum_{k \in \mathcal{K}} \alpha_k$ is non-increasing in each step of the admission control algorithm and the algorithm finally converges to a sub-optimal solution. \square

Lemma 2. *The Algorithm 4 of JPATO method converges after sufficient number of iterations.*

Proof. The joint optimization method in Algorithm 4 alternatively minimizes the objective function $\Psi(\xi, \mathbf{v}, \rho)$. Therefore, the value of the objective function does not increase in each step

of each iteration and converges after sufficient iterations. The convergence analysis of Algorithm 6 and Algorithm 7 involved in the disjoint method is equivalent to the one detailed for the previous algorithms based on joint method (not reported here due to the lack of space). \square

D. Summary of the proposed method

Herein we summarize the proposed algorithms in previous subsections. Algorithm 5 provides a quick view of Algorithm 3 and Algorithm 4 for the proposed admission control and joint optimization methods, respectively.

Algorithm 5: Summary of Algorithms 3 and 4.

Input: $\mathcal{K} = \{1, \dots, K\}$, $\alpha^0 = \Theta$ (very large), $\rho^0 = \epsilon$ (very small)

ξ^0 : random but compliant with C6

% Do the admission control

1 Solve (8) according to Algorithm 3, set $\xi^0 = \xi^{\text{ini}}$, $\rho^0 = \rho^{\text{ini}}$, $v^0 = v^{\text{ini}}$, and return \mathcal{K}^*

% Optimize the allocated resources for cost minimization

2 Solve (7) according to Algorithm 4

Output: ξ^* , ρ^* , v^*

E. Computational Complexity (CC) Analysis

In this section, we analyze CC of the proposed algorithms. CC of JPATO admission control algorithm is derived from the CC of solving the four subproblems and CC of the ASM modification algorithm. We adopt CVX solver for solving these subproblems in order to exploit IPM for finding the optimal solution [33]. Based on [34] and [35], the required number of iterations for IPM converge is given by $\frac{\log N_c}{\log \varsigma}$ where N_c is the total number of constraints, t^0 is the initial point for approximation of the barrier function, ϱ is the desired accuracy of convergence and $0 < \varsigma \ll 1$ is used for updating the stepsize of the barrier function accuracy. Therefore, CC of subproblems can be given as in Table II (a). Since we adopt CCP for solving the power allocation subproblem, we need to multiply CC of solving (18) by maximum permitted iterations of CCP, i.e., I_{\max}^p . Additionally, Algorithm 2 puts further CC on admission control algorithm. The required computations for calculation of the parameters in Algorithm 2 are provided in Table II (b) where B is the maximum number of the paths between any node and \bar{n} whereas

TABLE II: CC of solving different subproblems.

(a) CC of subproblems.		(b) CC of obtaining parameters in the ASM modification algorithm.	
Subproblems	Complexity	Parameter	Computational Complexity
Computational resource allocation (19)	$\frac{\log(2K+N)}{t^0 \varrho \log \varsigma}$	\mathcal{N}^k	$N \times E$
Power allocation (18)	$\frac{\log(2K+U+E)}{t^0 \varrho \log \varsigma}$	$\tilde{\Upsilon}_n^k$	$B \times (K-1)$
Task placement (20)	$\frac{\log(N+B+K)}{t^0 \varrho \log \varsigma}$	$\tilde{B}_{(m,m')}^k$	$N \times B \times (K-1)$
		(n^*, b^*)	$N \times B$

E is the total number of the edges in the network graph G . Hence, the CC of Algorithm 2 is $\mathcal{O}(K^2 \times N \times B \times E)$. CC of the admission control algorithm can be obtained by aggregating CC of all subproblems and Algorithm 2. More formally, we have:

$$CC^{\text{AC}} = K \times I_{\max} \left(\frac{\log(2K+N)}{t^0 \varrho \log \varsigma} + I_{\max}^{\rho} \times \frac{\log(2K+U+E)}{t^0 \varrho \log \varsigma} + \frac{\log(N+B+K)}{t^0 \varrho \log \varsigma} + \mathcal{O}(K^2 N B E) \right). \quad (26)$$

Similarly, the computational complexity of JPATO algorithm can be obtained as:

$$CC^{\text{JPATO}} = I_{\max} \left(\frac{\log(2K+N)}{t^0 \varrho \log \varsigma} + I_{\max}^{\rho} \times \frac{\log(2K+U+E)}{t^0 \varrho \log \varsigma} + \frac{\log(N+B+K)}{t^0 \varrho \log \varsigma} \right). \quad (27)$$

It can be seen that the CC of JPATO is of polynomial time in terms of network graph G parameters and the number of tasks K . As a result, the resource allocation can be performed by JPATO for larger networks with affordable computational cost.

VI. SIMULATION RESULTS

In this section, we evaluate the performance of the JPATO for admission control as well as joint task offloading and power allocation. The setup of our simulation is presented in Table III. We assume that $U = 4$ RRHs are placed with inter site distance of 100 m and all users are served in an area of 100 m radius with a given user-RRH assignment. The nodes of service providers' networks are generally divided in three tiers based on their distance from the end-users: the local tier, the regional tier, and the national tier. Although the number of serving nodes may be very large, there are some distant nodes in each tier that impose a large propagation delay. Hence, we only incorporate the nodes with reasonable propagation delay in the network graph [10]. The assumed network graph consists of $N = 6$ nodes: \bar{n} at the local tier with zero propagation delay, three nodes in the regional tier with relatively low propagation delay and two distant nodes at the national tier. For simplicity of comparison, we assume that all nodes have

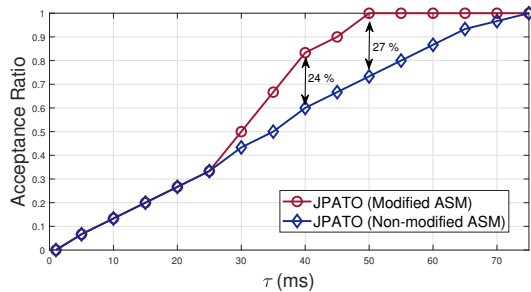
TABLE III: Simulation Setup.

Parameter	Value	Parameter	Value
L_k	10^6 CPU Cycles	$\delta_{(m,m')}$	10 ms
M	32 Antennas	$\gamma_{(m,m')}$	10^{-8} per bps
D_k	0.1 Mbits	Path Loss	$128.1 + 37.6 \log Q$ [22]
Υ_n	10^9 CPU Cycles per Second [7]	U	4
P_k^{\max}	0.5 Watt	ISD	100 m
$B_{(m,m')}$	0.4 Gbps	W	20 MHz [22]
$B_{f,u}$	0.6 Gbps	Noise power	-150 dBm/Hz [22]
Λ_n	10^{-28} [19]		

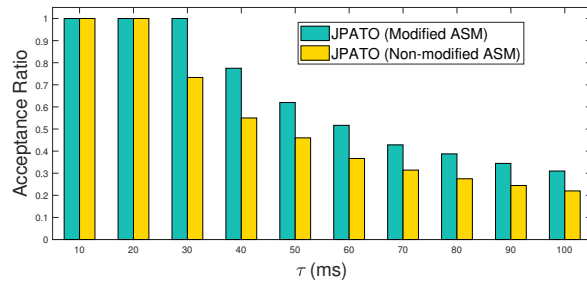
equal computational capacity and all tasks have equal size, load, and maximum tolerable latency. Moreover, we assume equal propagation delay and bandwidth for the network links. Note that the relatively low value of link bandwidth (0.4 Gbps) is the amount of bandwidth solely reserved to MEC tasks. Finally, the simulations are performed on a 3.30 GHz core i5 CPU and 16 GB RAM. Fig. 3 (a) reports the performance of admission control algorithm in JPATO, showing the acceptance ratio versus maximum tolerable latency of tasks. More in depth, the acceptance ratio is defined as the ratio of accepted services by the admission control algorithm over the total number of the requested tasks. By observing the figure, we can note that the acceptance ratio increases by increasing the maximum tolerable latency of tasks. This is due to the fact that the tasks with higher maximum tolerable latency need less resources (transmit power and computation) in order to be served. Moreover, for higher maximum tolerable latencies, there are more available nodes for tasks that can be offloaded. On the other hand, the effectiveness of the Alg. 2 can be seen in Fig. 3 (a). Interestingly, for latencies smaller than 75 ms, Alg. 2 outperforms the non-modified ASM algorithm. Moreover, the performance of the two methods is identical for low values of T . This is due to the fact that the set of accessible NFV-enabled nodes for low values of maximum tolerable latencies is restricted to \bar{n} and therefore, the modified ASM cannot offload the tasks to more distant NFV-enabled nodes because the corresponding propagation delay would tolerate the maximum tolerable latency of tasks.

The acceptance ratio of the JPATO admission control algorithm for different number of tasks is shown in Fig. 3 (b). Since the amount of available resources is limited, the acceptance ratio is decreasing with the increase in the total number of users. Again, the superiority of modified ASM over non-modified ASM can be observed.

The convergence of the JPATO admission control algorithm is shown in Fig. 4 (a). As expected, the sum of elasticization variables is decreasing in each iteration. Furthermore, it is shown that



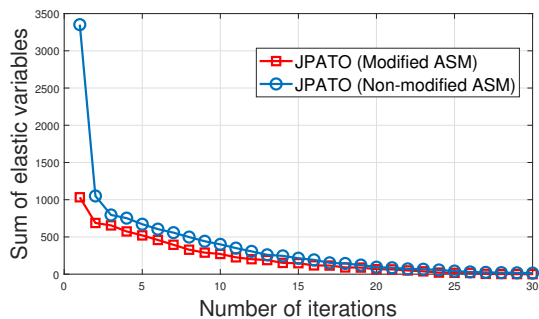
(a) Acceptance ratio vs. maximum tolerable latency for $K = 30$.



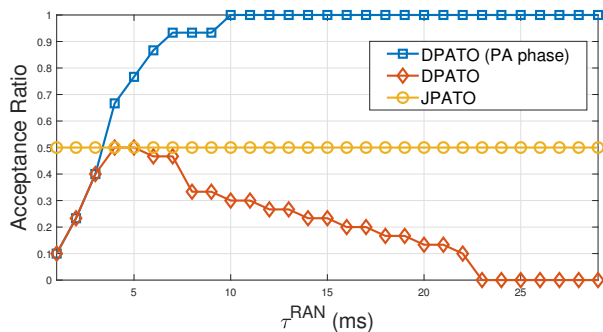
(b) Acceptance ratio vs. total number of tasks for $T = 40$ ms.

Fig. 3: Variations of acceptance ratio vs. maximum tolerable latency and number of tasks

the convergence of the modified ASM algorithm is faster than non-modified ASM algorithm which stems from higher acceptance ratio of modified ASM algorithm.



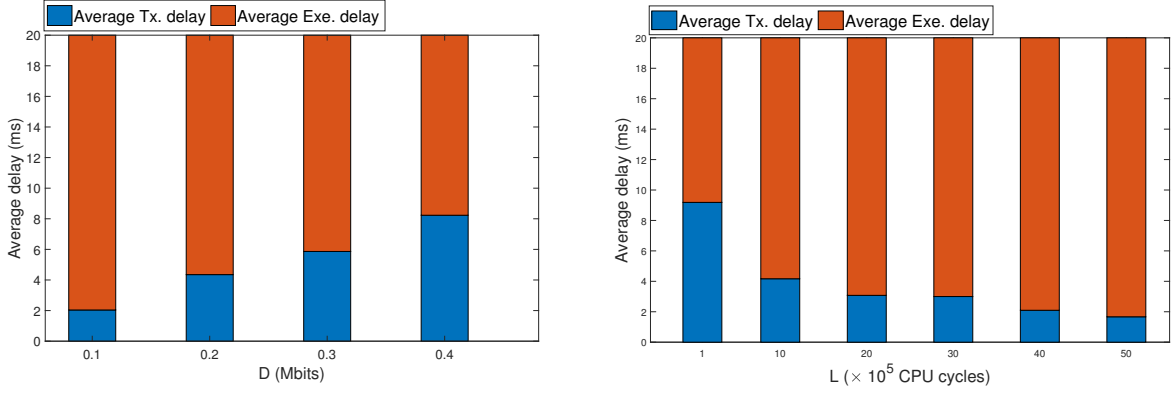
(a) Convergence of admission control algorithm for $T = 20$ ms and $K = 30$.



(b) Acceptance ratio of joint vs. disjoint methods in terms of T^{RAN} for $T = 30$ ms and $K = 30$ users.

Fig. 4: Performance of the proposed methods in terms of convergence and acceptance ratio.

In order to better position the performance of JPATO, we introduce the Disjoint Power Allocation and Task Offloading (DPATO) in Appendix A as the baseline of comparison. In DPATO, the radio part of the network has no information about the network graph and resources therein and vice-versa, a common assumption made in previous works [4]. Moreover, we should assume that the maximum tolerable latency of tasks is divided into two parts: T_k^{RAN} and $T_k - T_k^{\text{RAN}}$, where T_k^{RAN} is the part which is satisfied in radio domain and $T_k - T_k^{\text{RAN}}$ is satisfied in the network graph. The performance of the JPATO is compared with DPATO based on acceptance ratio criterion. In Fig. 4 (b), the acceptance ratio of the JPATO and the DPATO is depicted for the tasks with maximum tolerable latency of $T = T_k = 30$ ms. For DPATO, we



(a) Average delay of tasks transmission and execution delays in terms of data size D for $T = 20$ ms and $K = 30$. (b) Average delay of tasks transmission and execution delays in terms of tasks load L for $T = 20$ ms and $K = 30$.

Fig. 5: Average delay of tasks transmission and execution delays using JPATO.

obtain the acceptance ratio for different values of $T^{\text{RAN}} \in (0, T)$. Moreover, the acceptance ratio of admission control and power allocation algorithm is depicted. As it is shown in the figure, the acceptance ratio of DPATO is increasing for small values of T^{RAN} , that is, the small values of T^{RAN} impose high rates on users which can not be realized due to either interference or limited fronthaul capacity. On the other hand, for larger values of T^{RAN} , the acceptance ratio of the admission control and power allocation algorithm is 1 but the task offloading algorithm restricts the number of accepted tasks. Furthermore, it is observed that JPATO outperforms DPATO in different values of T^{RAN} . Fig. 5 (a) shows the average transmission delay of radio access network i.e., $\frac{1}{|\mathcal{K}|} \sum_{k \in \mathcal{K}} T_k^{\text{tx}}$ and the average execution delay of tasks, i.e., $\frac{1}{|\mathcal{K}|} \sum_{k \in \mathcal{K}} T_k^{\text{exe}}$ for different values of data size of tasks $D = D_k, \forall k$ and maximum tolerable latency $T = 20$ ms. As it can be observed, the average transmission delay increases by increasing the value of D , however, the average execution delay is decreased to maintain the maximum tolerable latency. Therefore, we can infer that the JPATO efficiently manages the radio resources and the computational resources for a successful task offloading. Similarly, the execution time of tasks increases by increasing the load of tasks. However, this increase can be compensated by lower transmission delay of the wireless link. Fig. 5 (b) shows the average transmission delay of the radio access network and the average execution delay of tasks for different values of tasks loads $L = L_k, \forall k$ and maximum tolerable latency $T = 20$ ms. In order to evaluate the performance of the JPATO, we assume there are three classes of tasks (each class consists of 10 tasks) with three different maximum tolerable latencies, i.e., $T^{(1)} = 10$ ms, $T^{(2)} = 50$ ms, and $T^{(3)} = 100$ ms. The classes (1), (2),

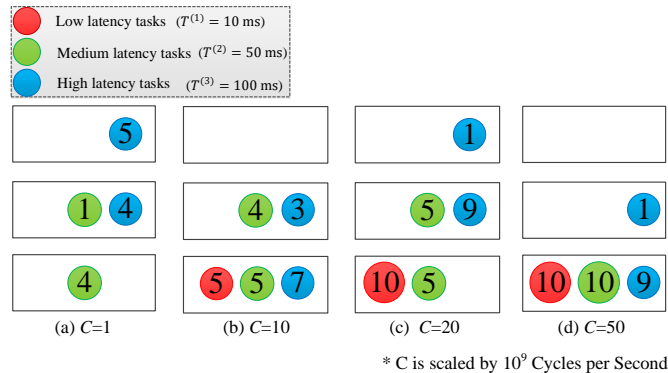


Fig. 6: Placement of the different classes of tasks at three different tiers of nodes for $K = 30$.

and (3) are considered as the sets of tasks with low, medium, and high latency requirement, respectively. Moreover, we assume there are three nodes (shown by rectangles in Fig. 6) with three different propagation delays, i.e., a local node (i.e., \bar{n}) with zero propagation delay, a regional node with 20 ms propagation delay, and a national node with 40 ms propagation delay. The propagation delays are assumed two-way, i.e., uplink+downlink propagation delays. Fig. 6 shows the task placement for different values of computational capacity of nodes $C = \Upsilon_n, \forall n$. As it is illustrated by Fig. 6, the nodes are not capable of serving class (1) of tasks due to their high resource utilization for $C = 1$, however, other two classes are served such that the tasks in class (2) are mainly served at local node and class (3) tasks are placed at regional and national node. By increasing the computational capacity to $C = 10$, some of the tasks in class (1) are placed at the local node. Moreover, some tasks in class (2) and (3) can be served at the local node as well. Furthermore, the national node does not serve any task because the JPATO tries to place the tasks at the nearest nodes in order to reduce the power consumption in the radio access network. When the computational capacity increases to $C = 20$, we observe that more tasks of class (1) are served at the local node and the acceptance ratio reaches to 1. By increasing even more the computational capacity to $C = 50$, almost all of tasks are placed at the local node in order to reduce the power consumption in the radio access network.

Table IV shows the acceptance ratio of each class for different values of computational capacity of nodes. It can be found out that the acceptance ratio of all classes is increased by increasing the computational capacity of nodes. Moreover, the acceptance ratio of class (1) is lower than that of classes (2) and (3). The reason is twofold, one is due to high resource utilization by tasks of this class and another is due to limited number of available nodes for tasks with low latency

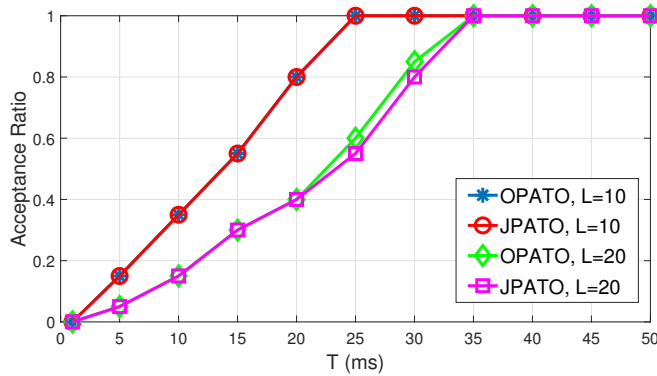


Fig. 7: Acceptance ratio of LPATO and JPATO vs. maximum tolerable latency.

requirement (only node \bar{n} in this example).

TABLE IV: Acceptance ratio of JPATO for different task classes w.r.t. computational capacity of nodes.

Computational capacity (10^9 CPU cycles/sec)	Maximum tolerable latency (ms)		
	$T^{(1)} = 10$	$T^{(2)} = 50$	$T^{(3)} = 100$
$C = 1$	0	0.5	0.9
$C = 10$	0.5	0.9	1
$C = 20$	1	1	1
$C = 50$	1	1	1

A lower bound on the optimal solution of power allocation and task offloading (LPATO) for optimization problem (8) is derived in Appendix B. The optimality gap of JPATO can be found in light of the performance comparison between JPATO with that of LPATO. Here, we compare the achieved acceptance ratio of JPATO with that of LPATO. Due to the high computational complexity of exhaustive search in LPATO, we consider a simple network graph comprised of two nodes connected with a single link. Moreover, the total number of tasks $|\mathcal{K}|$ is 20. Fig. 7 shows the acceptance ratio of LPATO and JPATO for different values of maximum tolerable latency T . The acceptance ratio of both JPATO and LPATO is lower for larger computational load. Meanwhile, the acceptance ratio of JPATO is almost the same as LPATO vs. the maximum tolerable latencies and computational loads.

VII. CONCLUSIONS AND FUTURE WORK

In this paper, we considered a task offloading problem in a cost-efficient manner while each task was constrained to a maximum tolerable latency. We investigated the joint impact of radio transmission, propagation of tasks through the transport network, and execution of tasks on the experienced latency of tasks. Due to the non-convexity of the optimization problem, we adopted the ASM which turned the optimization problem into: power allocation, task placement, and computational resource allocation subproblems. The power allocation was solved by adopting CCP to convexify the subproblem. The task placement and computational resource allocation were modeled as an ILP and convex subproblem, respectively. Moreover, we proposed a heuristic method based on ASM, with the goal of placing the tasks in more distant nodes when the computational resources are sufficient. Furthermore, to ensure the feasibility of optimization problem, we proposed an admission control mechanism to eliminate the tasks causing infeasibility. The simulation results showed the superiority of JPATO w.r.t. DPATO. The performance of the disjoint method depended on the part of latency required to be met in radio access network, i.e., T^{RAN} . However, the joint method showed higher acceptance ratio for different values of T^{RAN} . As future work, we plan to incorporate the task scheduling into JPATO. Moreover, the investigation of an innovative solution that divides the required computational load of each task among several nodes will be an interesting future research activity.

APPENDIX A

DISJOINT POWER ALLOCATION AND TASK OFFLOADING (DPATO)

In DPATO, the power allocation is decoupled from the task offloading optimization. The power allocation and task offloading optimization problems are similar to [22] and [4], respectively. Thus, the power allocation subproblem is solved first, and then we deal with the task offloading subproblem. The convexified version of the power allocation subproblem for the disjoint algorithm is given by:

$$\begin{aligned}
 & \min_{\boldsymbol{\rho}} \quad \sum_{k \in \mathcal{K}} \rho_k \\
 & \text{s.t.} \quad \text{C1-d: } h_k(\boldsymbol{\rho}) - \hat{g}_k(\boldsymbol{\rho}) \geq \frac{D_k}{T_k^{\text{RAN}}}, \quad \forall k \in \mathcal{K} \\
 & \quad \quad \text{C4-a, C5.}
 \end{aligned} \tag{28}$$

Again, we need an admission control mechanism to ensure the feasibility of this problem. Like the joint optimization problem, we adopt the elasticization approach. Therefore, similar to (18), the elasticized version of (28) can be stated as:

$$\begin{aligned} \min_{\boldsymbol{\rho}} \quad & 0 \\ \text{s.t.} \quad & \text{C1-e: } h_k(\boldsymbol{\rho}) - \hat{g}_k(\boldsymbol{\rho}) \geq \frac{D_k}{T_k^{\text{RAN}} + \alpha_k}, \quad \forall k \in \mathcal{K} \\ & \text{C4-a, C5,} \end{aligned} \quad (29)$$

which is solved via CCP. After the solution of (29), the elastic variables are updated as $\alpha_k = [T_k^{\text{tx}} - T_k^{\text{RAN}}]^+$ and then the task with maximum elastic variable is eliminated. This procedure is repeated until a feasible subset of tasks for power allocation obtained. After this step, subproblem (28) is solved according to the feasible subset of tasks. The disjoint admission control and power allocation method is shown in Algorithm 6. Given the power allocation solution, we solve the task offloading subproblem. The task offloading subproblem of disjoint algorithm is split into computational resource allocation and task placement steps. More formally, we have:

$$\begin{aligned} \min_{\mathbf{v}} \quad & \sum_{n \in \mathcal{N}} \sum_{k \in \mathcal{K}} \sum_{b \in \mathcal{B}_n} \Lambda_n \xi_{p_n^b}^k v_k^3 \\ \text{s.t.} \quad & \text{C1-f: } T_k^{\text{prop}} + \frac{L_k}{v_k} \leq T_k - T_k^{\text{RAN}}, \quad \forall k \in \mathcal{K}, \\ & \text{C2,} \end{aligned} \quad (30)$$

and

$$\begin{aligned} \min_{\boldsymbol{\xi}} \quad & \sum_{k \in \mathcal{K}} T_k^{\text{prop}} \\ \text{s.t.} \quad & \text{C1-f, C2, C3.} \end{aligned} \quad (31)$$

Similar to the power allocation algorithm, we need an admission control mechanism for the task offloading subproblem which can be achieved by elasticization. The elasticized versions of subproblems (30) and (31) are as follows:

$$\begin{aligned} \min_{\mathbf{v}} \quad & \sum_{k \in \mathcal{K}} T_k^{\text{exe}} \\ \text{s.t.} \quad & \text{C1-g: } T_k^{\text{prop}} + \frac{L_k}{v_k} \leq T_k - T_k^{\text{RAN}} + \alpha_k, \quad \forall k \in \mathcal{K} \\ & \text{C2,} \end{aligned} \quad (32)$$

and

$$\begin{aligned} \min_{\boldsymbol{\xi}} \quad & \sum_{k \in \mathcal{K}} T_k^{\text{prop}} \\ \text{s.t.} \quad & \text{C1-g: } T_k^{\text{prop}} \leq T_k - T_k^{\text{RAN}} + \alpha_k - T_k^{\text{exe}}, \quad \forall k \\ & \text{C2, C3, C6.} \end{aligned} \quad (33)$$

When the solutions of (32) and (33) are obtained, the elastic variables are updated by $\alpha_k = [T_k^{\text{exe}} + T_k^{\text{prop}} - T_k + T_k^{\text{RAN}}]^+$ and the algorithm continues until a feasible subset of constraints is achieved. The disjoint admission control and task offloading is shown in Algorithm 7.

Algorithm 6: Admission control and power allocation algorithm for disjoint method for solving (28) and (29).

Input: $\mathcal{K} = \{1, \dots, K\}, i = 0, \alpha^0 = \Theta$ (very large), $\rho^0 = \epsilon$ (very small),

$$T_k^{\text{RAN}} = (0, T_k), \forall k \in \mathcal{K}$$

```

1 repeat
2   repeat
3     % Allocate power to the users to minimize the sum of the transmission latencies
4     Solve (29) via CCP in Algorithm 1 and set  $\rho^{i+1} = \rho^*$ 
5     % Update the elastic variables
6      $s_k^{i+1} = [T_k^{\text{RAN}} - T_k^{\text{tx}}]^+, \quad \forall k \in \mathcal{K}$ 
7      $i = i + 1$ 
8   until  $\sum_{k \in \mathcal{K}} \alpha_k^{i-1} - \sum_{k \in \mathcal{K}} \alpha_k^i \leq \epsilon$  or  $i \geq I_{\max}$ 
9   % Find the task with maximum associated elastic variable
10   $k^* = \arg \max_{k \in \mathcal{K}} \alpha_k^i$ 
11  if  $\alpha_{k^*} > 0$  then
12    % Eliminate the task with maximum associated elastic variable
13     $\mathcal{K} = \mathcal{K} \setminus \{k^*\}$ 
14  else
15    break
16 until  $\sum_{k \in \mathcal{K}} \alpha_k = 0$ 
17 % Allocate power to the users with the cost minimization objective
18 Solve (28) via CCP in Algorithm 1 and return  $\rho^*$ 

```

Output: $\rho^*, \mathcal{K}^{\text{RAN}}$

APPENDIX B

A LOWER BOUND ON OPTIMAL SOLUTION

Since the optimization problem (8) is highly non-convex, some assumptions are made to resolve the non-convexity of (8), without loss of the optimality. First, we note that it is very likely for the fiber-optic links to have sufficient bandwidth for carrying the traffic of UEs, which is the case for fronthaul links and any wired link in the network G . As a result, we can relax the constraints C3 and C4 from (8). Note that the relaxation of C3 and C4 extends the feasible set of (8). As a result, LPATO may find a lower bound solution of (8). With a large number of antenna elements at RRHs, the lengths of random channel vectors are large. As a result, the

Algorithm 7: Admission control and task offloading algorithm of disjoint method for solving (30) - (33).

Input: \mathcal{K}^{RAN} , $i = 0$, $\alpha^0 = \Theta$ (very large), ξ^0 : random but compliant with C6

```

1 repeat
2   repeat
3     % Allocate computational resources to the tasks
4     Solve (32) and set  $\mathbf{v}^{i+1} = \mathbf{v}^*$ 
5     % Determine the node and the path for offloading the tasks
6     Solve (33) and set  $\xi^{i+1} = \xi^*$ 
7     % Update the elastic variables
8      $\alpha_k^{i+1} = [T_k - T_k^{\text{RAN}} - T_k^{\text{exe}} - T_k^{\text{prop}}]^+$ 
9     Update  $\mathbf{v}^{i+1}$ ,  $\xi^{i+1}$  and  $\alpha^{i+1}$  via the ASM modification algorithm (Algorithm 2)
10     $i = i + 1$ 
11  until  $\sum_{k \in \mathcal{K}} \alpha_k^{i-1} - \sum_{k \in \mathcal{K}} \alpha_k^i \leq \epsilon$  or  $i \geq I_{\max}$ 
12    % Find the task with maximum associated elastic variable
13     $k^* = \arg \max_{k \in \mathcal{K}} \alpha_k$ 
14    if  $\alpha_{k^*} > 0$  then
15      % Eliminate the task with maximum associated elastic variable
16       $\mathcal{K} = \mathcal{K} \setminus \{k^*\}$ 
17    else
18      break
19 until  $\sum_{k \in \mathcal{K}} \alpha_k = 0$ 
20 Set  $i = 0$ 
21 repeat
22   % Allocate computational resources to the tasks with the cost minimization objective
23   Solve (30) and set  $\mathbf{v}^{i+1} = \mathbf{v}^*$ 
24   % Determine the node and the path for offloading the tasks with the cost
25   minimization objective
26   Solve (31) and set  $\xi^{i+1} = \xi^*$ 
27 until  $\Psi(\xi^{i-1}, \mathbf{v}^{i-1}, \rho^*) - \Psi(\xi^i, \mathbf{v}^i, \rho^*) \leq \epsilon$  or  $i \geq I_{\max}$ 

```

Output: ξ^* , ρ^* , \mathbf{v}^* , $\mathcal{K}^{\text{Disjoint}}$

channel vectors between different RRHs and a specific user are approximately orthogonal, i.e., $|\mathbf{h}_{u,k}^H \mathbf{h}_{u,j}| \approx 0$ for all $j \neq k$ [36]. Therefore, the impact of interference in wireless channels is negligible and (14) becomes:

$$R_k = W \log_2 \left(1 + \frac{|\mathbf{h}_{u,k}|^2}{\sigma^2} \rho_k \right), \quad k \in \mathcal{K}_u. \quad (34)$$

The elimination of the interference increases R_k with the same amount of power allocated to each UE, which again leads to a lower bound solution of (8). Based on the fact that $\min_{\alpha, \xi, \mathbf{v}, \rho} \sum_{k \in \mathcal{K}} \alpha_k = \min_{\alpha, \xi, \mathbf{v}} \left(\min_{\rho} \sum_{k \in \mathcal{K}} \alpha_k \right)$, the optimal power allocation is the solution of:

$$\begin{aligned} & \min_{\rho} \sum_{k \in \mathcal{K}} \alpha_k \\ \text{s.t.} \quad & \text{C1: } T_k^{\text{exe}} + T_k^{\text{prop}} + T_k^{\text{tx}} \leq T_k + \alpha_k, \quad \forall k, \\ & \text{C5: } \rho_k \leq P_k^{\text{max}}, \quad \forall k. \end{aligned} \quad (35)$$

The data rate in (34) removes the cross-coupling impact of the allocated power to different users on constraint C1. Hence, without loss of optimality, (35) can be separately solved for each ρ_k independently. The associated power allocation problem is:

$$\begin{aligned} & \min_{\rho_k} T_k^{\text{tx}} \\ \text{s.t.} \quad & \text{C1: } T_k^{\text{exe}} + T_k^{\text{prop}} + T_k^{\text{tx}} \leq T_k + \alpha_k, \quad \forall k, \\ & \text{C5: } \rho_k \leq P_k^{\text{max}}, \quad \forall k, \end{aligned} \quad (36)$$

in which α_k in the objective is replaced with T_k^{tx} . Minimizing T_k^{tx} is equivalent to maximizing $\frac{R_k}{D_k}$. Since R_k in (34) is increasing with ρ_k , the optimal solution of (36) is $\rho_k^* = P_k^{\text{max}}$. Note that feasibility of C1 is ensured by optimizing other variables.

Next, we deal with the binary optimization variable ξ . We propose an exhaustive search over all possible values of ξ to avoid any performance loss due to non-convexity of (8), stemmed from binary ξ . All possible combinations of offloading decisions equals $|\mathcal{B}|^{|\mathcal{K}|}$ where $|\mathcal{B}| = \sum_n |\mathcal{B}_n|$. Thus, we solve (8) for α and \mathbf{v} for each offloading decision, and select the offloading decision resulting in lowest $\sum_k \alpha_k$ as the optimal offloading decision. For a typical network graph, the exhaustive search may impose an excessive computational complexity. However, LPATO is developed as a baseline for performance evaluation and it is not supposed to work in real-time.

The optimization problem for solving α and \mathbf{v} is:

$$\begin{aligned} & \min_{\mathbf{v}, \alpha} \sum_{k \in \mathcal{K}} \alpha_k \\ \text{s.t.} \quad & \text{C1-a: } \frac{L_k}{v_k} \leq \tilde{T}_k + \alpha_k, \quad \forall k \in \mathcal{K} \\ & \text{C2: } \sum_{k \in \mathcal{K}_n} v_k \leq \Upsilon_n, \quad \forall n, \end{aligned} \quad (37)$$

where $\tilde{T}_k = T_k - T_k^{\text{prop}} - T_k^{\text{tx}}$ and \mathcal{K}_n is the set of tasks to be executed in node n . Problem (37) is convex in both α and v . As a result, the KKT conditions determine the optimal solution. To derive the KKT conditions, we first write the Lagrangian function as follows:

$$\mathcal{L} = \sum_{k \in \mathcal{K}} \left(\alpha_k + \gamma_k \left(\frac{L_k}{v_k} - \tilde{T}_k - \alpha_k \right) - \eta_k \alpha_k - \mu_k v_k \right) + \sum_{n \in \mathcal{N}} \lambda_n \left(\sum_{k \in \mathcal{K}_n} v_k - \Upsilon_n \right). \quad (38)$$

By derivating Lagrange function with respect to α_k and v we have:

$$\frac{\partial \mathcal{L}}{\partial \alpha_k} = 1 - \gamma_k - \eta_k = 0, \quad \forall k \in \mathcal{K}, \quad (39)$$

and

$$\frac{\partial \mathcal{L}}{\partial v_k} = -\gamma_k \frac{L_k}{v_k^2} - \mu_k + \lambda_n = 0, \quad \forall k \in \mathcal{K}_n. \quad (40)$$

The complementary slackness conditions are:

$$\gamma_k \left(\frac{L_k}{v_k} - \tilde{T}_k - \alpha_k \right) = 0, \quad \forall k \in \mathcal{K}, \quad (41)$$

$$\lambda_n \left(\sum_{k \in \mathcal{K}_n} v_k - \Upsilon_n \right) = 0, \quad \forall n \in \mathcal{N}, \quad (42)$$

$$\eta_k \alpha_k = 0, \quad \forall k \in \mathcal{K}, \quad (43)$$

$$\mu_k v_k = 0, \quad \forall k \in \mathcal{K}. \quad (44)$$

The constraint C1-a implies $v_k > 0$. Hence, from (44) we have $\mu_k = 0$ and condition (40) results in:

$$v_k = \sqrt{\frac{L_k}{\lambda_n}}, \quad \forall k \in \mathcal{K}_n, \quad (45)$$

which implies $\lambda_n > 0$. Thus, (42) gives:

$$\sum_{k \in \mathcal{K}_n} v_k = \Upsilon_n, \quad \forall n \in \mathcal{N}. \quad (46)$$

On the other hand, when (7) is infeasible, we get $\alpha_k > 0$. Thus, (43) leads to $\eta_k = 0$ and condition (39) results in $\gamma_k = 1$. As a result, from (41) we get:

$$\alpha_k = \frac{L_k}{v_k} - \tilde{T}_k, \quad \forall k \in \mathcal{K}. \quad (47)$$

Having $\alpha_k \geq 0$ and (45), the optimal elastic variable is:

$$\alpha_k = [\sqrt{L_k \lambda_n} - \tilde{T}_k]^+, \quad \forall k \in \mathcal{K}_n, \quad (48)$$

wherein λ_n can be found such that:

$$\sum_{k \in \mathcal{K}_n} \frac{L_k}{\bar{T}_k + \alpha_k} = \Upsilon_n, \quad \forall n \in \mathcal{N}. \quad (49)$$

Then, the optimal values of α_k and v_k can be found as in (48) and (45), respectively. Having the optimal solution of (37) for all possible ξ , the optimal solution of (8) is the solution with lowest objective of (37).

REFERENCES

- [1] B. Yi, X. Wang, K. Li, S. K. Das, and M. Huang, "A comprehensive survey of network function virtualization," *Computer Networks*, vol. 133, pp. 212–262, 2018.
- [2] P. Mach and Z. Becvar, "Mobile edge computing: A survey on architecture and computation offloading," *IEEE Communications Surveys & Tutorials*, vol. 19, no. 3, pp. 1628–1656, 2017.
- [3] ETSI, "Mobile Edge Computing (MEC); Framework and reference architecture," *ETSI Group Specification MEC 003*, 2016.
- [4] B. Yang, W. K. Chai, Z. Xu, K. V. Katsaros, and G. Pavlou, "Cost-efficient NFV-enabled mobile edge-cloud for low latency mobile applications," *IEEE Transactions on Network and Service Management*, vol. 15, no. 1, pp. 475–488, 2018.
- [5] T. Li, C. S. Magurawalage, K. Wang, K. Xu, K. Yang, and H. Wang, "On efficient offloading control in cloud radio access network with mobile edge computing," in *2017 IEEE 37th International Conference on Distributed Computing Systems (ICDCS)*, pp. 2258–2263, IEEE, 2017.
- [6] H. Guo, J. Liu, and J. Zhang, "Computation offloading for multi-access mobile edge computing in ultra-dense networks," *IEEE Communications Magazine*, vol. 56, no. 8, pp. 14–19, 2018.
- [7] L. Yang, H. Zhang, M. Li, J. Guo, and H. Ji, "Mobile edge computing empowered energy efficient task offloading in 5G," *IEEE Transactions on Vehicular Technology*, vol. 67, no. 7, pp. 6398–6409, 2018.
- [8] M.-H. Chen, M. Dong, and B. Liang, "Resource sharing of a computing access point for multi-user mobile cloud offloading with delay constraints," *IEEE Transactions on Mobile Computing*, vol. 17, no. 12, pp. 2868–2881, 2018.
- [9] W. Almughalles, R. Chai, J. Lin, and A. Zubair, "Task execution latency minimization-based joint computation offloading and cell selection for MEC-enabled HetNets," in *2019 28th Wireless and Optical Communications Conference (WOCC)*, pp. 1–5, IEEE, 2019.
- [10] T. X. Tran and D. Pompili, "Joint task offloading and resource allocation for multi-server mobile-edge computing networks," *IEEE Transactions on Vehicular Technology*, vol. 68, no. 1, pp. 856–868, 2019.
- [11] T. Q. Dinh, J. Tang, Q. D. La, and T. Q. Quek, "Offloading in mobile edge computing: Task allocation and computational frequency scaling," *IEEE Transactions on Communications*, vol. 65, no. 8, pp. 3571–3584, 2017.
- [12] X. Chen, L. Jiao, W. Li, and X. Fu, "Efficient multi-user computation offloading for mobile-edge cloud computing," *IEEE/ACM Transactions on Networking*, vol. 24, no. 5, pp. 2795–2808, 2015.
- [13] K. Zhang, Y. Mao, S. Leng, Q. Zhao, L. Li, X. Peng, L. Pan, S. Maharjan, and Y. Zhang, "Energy-efficient offloading for mobile edge computing in 5G heterogeneous networks," *IEEE access*, vol. 4, pp. 5896–5907, 2016.
- [14] P. Zhao, H. Tian, C. Qin, and G. Nie, "Energy-saving offloading by jointly allocating radio and computational resources for mobile edge computing," *IEEE Access*, vol. 5, pp. 11255–11268, 2017.

- [15] X. Zhang, Y. Mao, J. Zhang, and K. B. Letaief, "Multi-objective resource allocation for mobile edge computing systems," in *2017 IEEE 28th Annual International Symposium on Personal, Indoor, and Mobile Radio Communications (PIMRC)*, pp. 1–5, IEEE, 2017.
- [16] J. Zhang, X. Hu, Z. Ning, E. C.-H. Ngai, L. Zhou, J. Wei, J. Cheng, and B. Hu, "Energy-latency tradeoff for energy-aware offloading in mobile edge computing networks," *IEEE Internet of Things Journal*, vol. 5, no. 4, pp. 2633–2645, 2017.
- [17] C. Wang, F. R. Yu, C. Liang, Q. Chen, and L. Tang, "Joint computation offloading and interference management in wireless cellular networks with mobile edge computing," *IEEE Transactions on Vehicular Technology*, vol. 66, no. 8, pp. 7432–7445, 2017.
- [18] C. You, K. Huang, H. Chae, and B.-H. Kim, "Energy-efficient resource allocation for mobile-edge computation offloading," *IEEE Transactions on Wireless Communications*, vol. 16, no. 3, pp. 1397–1411, 2016.
- [19] F. Zhou, Y. Wu, R. Q. Hu, and Y. Qian, "Computation rate maximization in UAV-enabled wireless-powered mobile-edge computing systems," *IEEE Journal on Selected Areas in Communications*, vol. 36, no. 9, pp. 1927–1941, 2018.
- [20] A. Khalili, S. Zarandi, and M. Rasti, "Joint resource allocation and offloading decision in mobile edge computing," *IEEE Communications Letters*, vol. 23, no. 4, pp. 684–687, 2019.
- [21] J. Zhang, W. Xia, F. Yan, and L. Shen, "Joint computation offloading and resource allocation optimization in heterogeneous networks with mobile edge computing," *IEEE Access*, vol. 6, pp. 19324–19337, 2018.
- [22] W. Xia, J. Zhang, T. Q. Quek, S. Jin, and H. Zhu, "Power minimization-based joint task scheduling and resource allocation in downlink C-RAN," *IEEE Transactions on Wireless Communications*, vol. 17, no. 11, pp. 7268–7280, 2018.
- [23] S. Li, N. Zhang, S. Lin, L. Kong, A. Katangur, M. K. Khan, M. Ni, and G. Zhu, "Joint admission control and resource allocation in edge computing for internet of things," *IEEE Network*, vol. 32, no. 1, pp. 72–79, 2018.
- [24] J. Guo, Z. Song, Y. Cui, Z. Liu, and Y. Ji, "Energy-efficient resource allocation for multi-user mobile edge computing," in *GLOBECOM 2017-2017 IEEE Global Communications Conference*, pp. 1–7, IEEE, 2017.
- [25] M.-H. Chen, B. Liang, and M. Dong, "Joint offloading decision and resource allocation for multi-user multi-task mobile cloud," in *2016 IEEE International Conference on Communications (ICC)*, pp. 1–6, IEEE, 2016.
- [26] A. Al-Shuwaili and O. Simeone, "Energy-efficient resource allocation for mobile edge computing-based augmented reality applications," *IEEE Wireless Communications Letters*, vol. 6, no. 3, pp. 398–401, 2017.
- [27] Y. Yu, J. Zhang, and K. B. Letaief, "Joint subcarrier and cpu time allocation for mobile edge computing," in *2016 IEEE Global Communications Conference (GLOBECOM)*, pp. 1–6, IEEE, 2016.
- [28] J. Liu, Y. Mao, J. Zhang, and K. B. Letaief, "Delay-optimal computation task scheduling for mobile-edge computing systems," in *2016 IEEE International Symposium on Information Theory (ISIT)*, pp. 1451–1455, IEEE, 2016.
- [29] J. Li, H. Gao, T. Lv, and Y. Lu, "Deep reinforcement learning based computation offloading and resource allocation for MEC," in *2018 IEEE Wireless Communications and Networking Conference (WCNC)*, pp. 1–6, IEEE, 2018.
- [30] J. W. Chinneck, *Feasibility and Infeasibility in Optimization*. Algorithms and Computational Methods, Springer, 2008.
- [31] T. Lipp and S. Boyd, "Variations and extension of the convex–concave procedure," *Optimization and Engineering*, vol. 17, no. 4, pp. 263–287, 2016.
- [32] MOSEK ApS, *The MOSEK optimization toolbox for MATLAB manual. Version 9.0.*, 2019.
- [33] CVX Research, Inc., "CVX: Matlab software for disciplined convex programming." <http://cvxr.com/cvx>, 2017.
- [34] N. Mokari, F. Alavi, S. Parsaefard, and T. Le-Ngoc, "Limited-feedback resource allocation in heterogeneous cellular networks," *IEEE Transactions on Vehicular Technology*, vol. 65, pp. 2509–2521, April 2016.
- [35] S. Boyd and L. Vandenberghe, *Convex Optimization*. New York, NY, USA: Cambridge University Press, 2004.
- [36] L. Lu, G. Y. Li, A. L. Swindlehurst, A. Ashikhmin, and R. Zhang, "An overview of massive MIMO: Benefits and challenges," *IEEE journal of selected topics in signal processing*, vol. 8, no. 5, pp. 742–758, 2014.